X 90-36005

X90-36005

NASA Technical Memorandum 4162

Effect of Pylon Wake With and Without Pylon Blowing on Propeller Thrust

Garl L. Gentry, Jr., Earl R. Booth, Jr.,
and M. A. Takallu

FEBRUARY 1990

NASA

NASA Technical Memorandum 4162

Effect of Pylon Wake With and Without Pylon Blowing on Propeller Thrust

Garl L. Gentry, Jr., and Earl R. Booth, Jr.
Langley Research Center
Hampton, Virginia

M. A. Takallu
PRC Kentron, Inc.
Aerospace Technologies Division
Hampton, Virginia

NASA
National Aeronautics and
Space Administration
Office of Management
Scientific and Technical
Information Division

1990

Summary

Pylon trailing-edge blowing has been investigated as a means of alleviating the effects of the pylon wake on a pusher arrangement of an advanced single-rotation turboprop. Measurements were made of the steady-state propeller thrust and pylon-wake pressure distribution and turbulence level with and without blowing. Results showed pylon trailing-edge blowing practically eliminated the pylon wake, significantly reduced the pylon-wake turbulence, and had a relatively small effect on the steady-state propeller thrust. The data are presented with a minimum of analysis.

Introduction

Studies of next-generation passenger aircraft point to the use of an advanced turboprop for propulsion (ref. 1). The new turboprop configurations promise a significant fuel savings over current-generation turbofan-powered aircraft (refs. 2 and 3).

However, advanced turboprop aircraft are not without their problems. The Advanced Turboprop (ATP) aircraft are expected to be noisier than current-generation turbofan aircraft, and the noise they produce will be tonal in nature which may be more annoying both to the passenger in the aircraft and to the community in the vicinity of the airport. In addition, the large diameter of the turboprops and the vibration levels induced on the fuselage in the propeller plane make wing-mounted nacelles less practical (ref. 4). As a result, most of the design proposals employing ATP propulsion place the turboprop nacelle on a pylon extending from the aft fuselage. Such designs can be divided into two categories—tractor and pusher configurations, where the propeller is mounted in front of or behind the support pylon, respectively.

Tractor configurations have a primary disadvantage in that they position the propeller plane closer to the passenger cabin than pusher configurations, thereby partially defeating the purpose of mounting the support pylon on the aft fuselage. In addition, the propeller wake impinges on the pylon, thus transmitting vibration to the aircraft (ref. 4).

Pusher configurations have the advantage of placing the propeller plane farthest from the passenger cabin, and then the propeller wake does not impinge directly on the aircraft. However, since the propeller is located downstream of the support pylon, the propeller inflow is distorted by the pylon wake (ref. 5). This inflow distortion results in a time-dependent variation of thrust as each blade passes through the pylon wake. The harmonic nature of this thrust variation can cause increased vibratory loads on the blades and engine mounting and these loads can be transmitted to the aircraft fuselage (ref. 4). Additionally, the transient loading on blade surfaces will decrease blade fatigue life (ref. 6) and will increase noise generation (ref. 7). Although the aforementioned research and other efforts (such as ref. 8) have focused on the influence of inflow distortions, little research has been published on methods of alleviating these adverse wake effects on advanced turboprops. The present experiment was designed to address this need as part of the NASA Advanced Turboprop program. The NASA ATP program is developing a data base to support effective configuration integration of advanced turboprop concepts.

A simple experiment was designed using a model turboprop operating in the wake of a model pylon/nacelle system that was designed to incorporate blowing slots at the trailing edge. Measurements of the pylon-wake pressure distribution and turbulence level were made with and without blowing for two slot spans. The performance of the propeller was measured in terms of time-averaged thrust coefficient. The objectives of this test were to measure the feasibility of using trailing-edge blowing to obtain a uniform pylon wake into the turboprop and to determine the propeller performance in the presence of the pylon both with and without blowing.

Symbols

a	local speed of sound, ft/sec
b	pylon semispan, 54.75 in.
C_p	total pressure coefficient, $(p - p_\infty)/q_\infty$
C_T	propeller thrust coefficient, $T/\rho n^2 d^4$
c	pylon chord (14 in.)
d	diameter
J	propeller advance ratio, U_∞/nd
M_t	propeller-tip Mach number, $\pi nd/a$
N_{Re}	Reynolds number, 1/ft
n	propeller rotational velocity, rps or rpm
PCA	pitch change axis
p	pylon-wake pressure, psf
p_∞	free-stream static pressure, psf
q_∞	tunnel free-stream dynamic pressure, psf
R	blade radius, in.

r	blade radial station, in.
s	distance between trailing edge of pylon and PCA, in.
T	axial force, lb
U_∞	free-stream velocity, ft/sec
u'	flow perturbation velocity, ft/sec
y	distance along semispan from root to tip, in.
z	distance normal to pylon, in.
$\beta_{.75}$	propeller blade-inclination angle at 0.75 radial station, deg
η	spanwise coordinate, y/b
ρ	density, slugs/ft^3

Experimental Apparatus

The investigation was conducted in the Langley 14- by 22-Foot Subsonic Tunnel, which has a test section 14.50 ft high, 21.75 ft wide, and 50 ft long. This is a closed-circuit atmospheric wind tunnel with a test-section speed variable up to 200 knots.

An overall view of the experimental setup is shown in figure 1, and dimensional information is provided in table I. The model consists of a rectangular planform pylon with a 14-in. chord, an NACA 0012 airfoil section, and an eight-blade, single-rotation propeller driven by an air turbine motor. The model was constructed with the pylon/nacelle system and motor supported separately to allow testing of the propeller both alone and in the pylon/nacelle wake. In this manner, the magnitude of performance change associated with propeller operation in the pylon/nacelle wake could be directly assessed. The pylon model had a spanwise slot at the 80-percent-chord location for controlled airflow blowing at the trailing edge. The trailing-edge blowing was used to add mass to the airfoil wake and reduce the velocity deficit, thus creating a more uniform inflow for a pusher propeller system. A sketch of the pylon cross section is presented showing the arrangement of the internal pressure plenum, flow slot, and trailing-edge fairing (fig. 2).

The propeller was a 1-ft-diameter model of the SR-7 turboprop geometrically described in reference 6. The propeller was driven by an air turbine motor capable of producing 120 hp at 16 000 rpm with a design maximum of 19 000 rpm. Motor rotational speed (rpm) was measured using a 30-per-revolution signal decoded by a tachometer. The motor was operated to approximately 15 000 rpm during the test. Propeller disk loads were monitored using an integrally mounted strain-gauge balance. The data presented herein are derived from time-averaged balance readings.

Test Measurements and Conditions

The isolated propeller and the propeller installed in the wake of the pylon with and without slot blowing were each tested at three dynamic pressures: 20, 30, and 40 psf. Two blowing configurations were tested. (See table II.) In configuration 1 the blowing slot extended from $\eta = 0.82$ to $\eta = 0.96$ (the pylon/nacelle juncture). In configuration 2 the blowing slot extended from $\eta = 0.82$ to $\eta = 0.92$. These slot lengths provided pylon-wake blowing extending from $r/R = 0.33$ to $r/R = 1.64$ and from $r/R = 0.75$ to $r/R = 1.64$, respectively. Propeller blade angles were set to geometrical angles of 25° and 40° at the 0.75 radial blade station. No attempt was made to measure blade angle under load. For all tests the turboprop model was mounted at zero angle of attack. The propeller rpm was varied to obtain a range of advance ratios at each dynamic pressure.

The total pressure distribution of the wake produced by the isolated pylon was measured in the plane normal to the pylon span at the 0.75 radial blade station of the propeller pitch change axis. The total pressure rake shown in figure 3 had 50 total pressure tubes spaced 0.1 in. apart to survey an area 5 in. wide. The pylon wake was surveyed at numerous spanwise locations to determine spanwise uniformity of the pylon wake. The data were normalized by the free-stream dynamic pressure and plotted as a function of spanwise location. Presented in this manner, the data show a three-dimensional picture of the wake produced by the pylon. Measurements were made for various pylon blowing rates until a condition of minimum total pressure loss was obtained for each free-stream velocity used in the experiment. The resulting operating conditions were used for subsequent evaluation of the blown pylon concept. In addition, the mean turbulence level of the pylon wake was measured using a hot-wire probe. The one-dimensional turbulence intensity u'/U_∞ was directly measured for both the blowing case and the no-blowing case to evaluate the flow quality produced by the slot flow.

Discussion of Results

The results obtained for the propeller in isolation, the propeller with pylon, and the propeller with pylon blowing for two different blowing configurations are listed in table III. These results are documented according to designated run numbers for each tunnel dynamic pressure, as shown in table II.

Pylon-Wake Measurements

The results of the pylon-wake measurements with and without slot blowing are presented in figures 4 to 11 for the range of dynamic pressures tested. Figure 4 consists of the pylon-wake total pressure surveys of configuration 1 at $q_\infty = 20$ psf both with and without pylon blowing for $\eta = 0.82$ to 0.96. This corresponds to $r/R = 0.33$ to 1.64 from the center of the propeller disk. Figure 4 shows that the velocity deficit with blowing is nearly zero from $\eta = 0.82$ to 0.93. Figures 5 and 6 show that this trend continues and actually improves with the increase in dynamic pressure.

For configuration 2 a block was inserted into the pylon slot so that there was no pylon blowing over the propeller inboard of $r/R = 0.75$, with the rationale that blowing would be most beneficial to the outboard 25 percent of the propeller where rotational velocities are highest. Figure 7 contains the pylon-wake total pressure surveys for configuration 2. Here, the velocity deficit is shown to be substantially reduced over the entire slot span, although, as expected, the data nearer the pylon/nacelle juncture show a small residual velocity deficit. As was the case with configuration 1, velocity deficit control becomes better with increasing dynamic pressure. (See figs. 7, 8, and 9.)

Figure 10 presents the one-dimensional wake turbulence intensity u'/U_∞ with and without pylon blowing at dynamic pressures of 20, 30, and 40 psf. The turbulence level of the wake for configuration 1 is approximately 9 percent without the pylon blowing and approximately 5 percent with the pylon blowing. Results for configuration 2 in figure 11 show a greater reduction in turbulence intensity when blowing is activated.

Isolated Propeller Performance

The results of isolated propeller performance are presented as the variation of thrust coefficient with propeller advance ratio. Figure 12 compares the experimental data for the isolated propeller with the data of reference 9 and with presently unpublished in-house predictions by Takallu. This figure shows the typical performance of this propeller for a pitch setting of 40° at the 0.75 radial station. Both the data of reference 9 and Takallu's prediction compare well with the present results. The effect of Reynolds number on the isolated propeller performance is presented in figures 13 and 14 as obtained from the three dynamic pressure conditions. Results for a blade angle of $\beta_{.75} = 40°$ in figure 13 show rather small variations with Reynolds number uniformly over the advance ratio range tested. Increased thrust is obtained at the highest Reynolds number. Essentially no Reynolds number dependency is evident for the $\beta_{.75} = 25°$ blade angle results shown in figure 14 where the blades are operating at a far lower thrust loading.

Installed Propeller Performance

The installed performance of the turboprop behind the pylon/nacelle system is presented in figures 15 to 18 and shows the influence of the pylon, the blowing slot configuration, and the blade angle.

The dominant effect shown in the data, particularly at higher advance ratios, is that the installed thrust levels (without blowing) are generally higher than the isolated levels. One might expect this result based on several factors. The pylon/nacelle wake reduces the inflow to the propeller at a specific advance ratio and pushes the blades to higher angles of attack resulting in increased thrust. Also, some reduction in drag force on the propeller balance is expected from the shielding of the hub by the nacelle. Finally, some modest increase in blade performance may be provided if a higher effective Reynolds number is provided by the wake turbulence. (The results of fig. 13 show a small Reynolds number effect.) In any case, these results show that the time-averaged propeller thrust registers a substantial favorable installation effect.

The influence of pylon blowing was found to have a relatively small impact when assessed in terms of time-averaged thrust coefficient. For slot configuration 1 (shown in figs. 15 and 16), the influence of blowing was small for both blade angles. For slot configuration 2 (shown in figs. 17 and 18), a larger effect was evident for the 40° blade setting at the higher advance ratios; the influence for the 25° blade setting is not measurable for slot configuration 2. (See fig. 18.) Indeed, for the configurations studied, the largest change in thrust was caused by the installation of the pylon/nacelle system and not by the addition of the slot blowing. If one assumes that the influence of the pylon on the propeller is substantially reduced for the pylon blowing condition, then it is apparent that the nacelle wake influence on the propeller performance is what remains. This is indeed substantial and, for the present experiment, appears to dominate the installation effects on propeller thrust performance. However, the effectiveness of pylon blowing, although masked by the nacelle wake effects in the steady-state thrust, may be evident in future tests if dynamic measurements of propeller thrust are made.

Another possibility is that blowing rates sufficient to reduce the velocity deficit behind the isolated pylon are insufficient to alleviate the wake when the

thrusting propeller is installed. However, the results noted in reference 8 indicate that the propeller did not have a very strong effect on the upstream wake. Future experiments being considered will obtain time-dependent thrust and power measurements to provide a complete picture of the propeller performance.

A complete assessment of the benefits of this pylon blowing concept will require that future experiments be conducted using both a quieter simulator and larger blades to ensure a sufficient dominance of the blade noise signature. An attractive experiment might incorporate larger blades to simulate accurately the blade geometry and allow the installation of dynamic blade-surface pressure measurements on the turboprop blades to define the unsteady blade loads directly for correlation with acoustic measurements.

Concluding Remarks

An experimental investigation was conducted for a scale model of the SR-7 turboprop to explore the use of pylon blowing to alleviate wake effects on propeller steady-state thrust performance. Two arrangements of slot blowing at the trailing edge of a pylon/nacelle system were investigated and both provided a substantial reduction in the pylon-wake deficit and turbulence. Although the pylon blowing produced noticeable improvements in the pylon-wake velocity deficit and turbulence level, only minor influences were noticed in the propeller thrust performance, with the largest effect (a small increase in thrust) being observed for the use of blowing applied only to the blade outer radius for the higher blade setting (40°). The influence of installing the turboprop behind the pylon/nacelle system was substantial and caused an increase in thrust coefficient that was most evident for high advance ratios. According to thrust coefficient measurements, installation of the nacelle on the turboprop had a more dominant effect than the pylon wake.

NASA Langley Research Center
Hampton, VA 23665-5225
December 15, 1989

References

1. Dunham, Dana Morris; Gentry, Garl L.; Manuel, Gregory S.; Applin, Zachary T.; and Quinto, P. Frank: *Low-Speed Aerodynamic Characteristics of a Twin-Engine General Aviation Configuration With Aft-Fuselage-Mounted Pusher Propellers.* NASA TP-2763, 1987.
2. Whitlow, J. B., Jr.; and Sievers, G. K.: *Fuel Savings Potential of the NASA Advanced Turboprop Program.* NASA TM-83736, [1984].
3. Smith, Bruce A.: Douglas Initiates Marketing Efforts To Promote MD-90 Propfan Program. *Aviation Week & Space Technol.,* vol. 129, no. 4, Jan. 25, 1988, pp. 38–39, 42.
4. Martinez, Rudolph: *Predictions of Unsteady Wing and Pylon Forces Caused by Propeller Installation.* NASA CR-178298, 1987.
5. Takallu, M. A.; and Spence, P. L.: Prediction of Unsteady Thrust and Torque Coefficients for a Pusher Propeller. AIAA-87-2630-CP, Aug. 1987.
6. Billman, L. C.; Gruska, C. J.; Ladden, R. M.; Leishman, D. K.; and Turnberg, J. E.: *Large Scale Prop-Fan Structural Design Study. Volume II—Preliminary Design of SR-7.* NASA CR-174993, [1988].
7. Takallu, M. A.; and Block, P. J. W.: Prediction of Added Noise Due to the Effect of Unsteady Flow on Pusher Propellers. AIAA-87-0255, Jan. 1987.
8. Simonich, J. C.; McCormick, D. C.; and Lávrich, P. L.: Interaction Noise Mechanisms for Advanced Propeller Experimental Results. AIAA-89-1093, Apr. 1989.
9. Aljabri, A. S.: Wind Tunnel Tests on a One-Foot Diameter SR-7L Propfan Model. AIAA-87-1892, June-July 1987.

Table I. Hardware Characteristics

Propeller:
- Diameter, d, in. 12
- Maximum chord, in. 14
- Hub diameter, in. 2.988

Nacelle:
- Maximum diameter, in. 4
- Length, nose to PCA, at $s = 0.1574c$, in. 22.70

Pylon:
- Chord length, c, in. 14
- Maximum thickness, in. 1.68
- Trailing edge to PCA, in. 2.20
- Slot height, in. 0.01

Table II. Test Matrix

Run	Blade angle at 0.75 radius, deg	Dynamic pressure, psf	Model setup
103	25	20	Isolated (nonblowing)
104	25	30	
105	25	40	
100	40	20	
101	40	30	
102	40	40	
166	25	20	Propeller and pylon (nonblowing)
164	25	30	
162	25	40	
111	40	20	
109	40	30	
107	40	40	
165	25	20	Propeller and pylon blowing (configuration 1)
163	25	30	
161	25	40	
110	40	20	
108	40	30	
106	40	40	
141	25	20	Propeller and pylon blowing (configuration 2)
140	25	30	
139	25	40	
138	40	20	
137	40	30	
136	40	40	

Table III. Tabulated Data

n, rpm	M_t	J	C_T
Run 100			
5 522	0.2581	1.4244	0.4680
7 090	.3313	1.1128	.5877
7 758	.3625	1.0171	.6174
8 792	.4107	.8950	.6351
9 246	.4320	.8535	.6470
9 782	.4570	.8068	.6603
10 570	.4961	.7452	.6745
12 244	.5748	.6414	.6986
14 594	.6851	.5427	.7095
Run 101			
6 838	0.3194	1.4117	0.4118
8 758	.4091	1.1043	.5507
9 454	.4416	1.0230	.5811
10 728	.5011	.9016	.6242
11 418	.5333	.8503	.6447
12 064	.5634	.8048	.6602
12 936	.6076	.7421	.6745
14 828	.6966	.6485	.7008
Run 102			
8 042	0.3754	1.3888	0.4323
9 900	.4621	1.1300	.5403
10 678	.4984	1.0478	.5748
12 436	.5805	.8996	.6307
12 434	.5804	.8997	.6355
13 094	.6112	.8556	.6494
13 990	.6531	.7996	.6681
14 984	.7043	.7414	.6938
Run 103			
3 158	0.1480	1.1109	0.1627
5 382	.2523	1.1249	.0696
6 898	.3234	1.1366	.0684
7 640	.3582	1.0263	.1386
8 712	.4085	.8999	.2089
9 118	.4275	.8599	.2304
9 714	.4554	.8071	.2561
10 510	.4951	.7424	.2862
12 382	.5833	.6320	.3367
14 728	.6939	.5328	.3833
15 902	.7493	.4962	.4019
Run 104			
8 536	0.4002	1.1310	0.0323
9 372	.4393	1.0302	.0994
10 604	.4971	.9122	.1750
10 850	.5087	.8915	.1897
11 298	.5296	.8545	.2098
11 998	.5625	.8031	.2409
12 874	.6070	.7427	.2701
15 018	.7082	.6379	.3216
15 858	.7477	.6041	.3394

Table III. Continued

n, rpm	M_t	J	C_T
Run 105			
10 112	0.4739	1.1004	0.0420
10 986	.5148	1.0129	.1012
12 216	.5724	.9122	.1643
13 060	.6119	.8521	.2034
13 828	.6479	.8059	.2318
14 886	.7022	.7447	.2623
15 808	.7457	.7002	.2839
Run 106			
7 858	0.3698	1.4162	0.4517
9 996	.4704	1.1087	.5611
10 908	.5133	1.0189	.5927
12 166	.5724	.9137	.6216
13 096	.6161	.8501	.6408
13 796	.6491	.8034	.6556
14 876	.7045	.7423	.6775
15 846	.7505	.6959	.6935
Run 107			
7 778	0.3659	1.4271	0.4493
9 768	.4595	1.1364	.5482
10 836	.5098	1.0258	.5877
12 318	.5796	.8998	.6308
13 032	.6131	.8519	.6482
13 866	.6523	.8006	.6657
14 238	.6744	.7744	.6817
14 964	.7086	.7380	.6989
15 730	.7449	.6980	.7103
Run 108			
6 798	0.3209	1.4091	0.4748
8 578	.4047	1.1192	.5683
9 408	.4439	1.0145	.5987
10 610	.5005	.9068	.6269
11 310	.5335	.8508	.6424
11 860	.5594	.8083	.6540
12 322	.5844	.7736	.6622
12 886	.6112	.7411	.6683
15 128	.7174	.6350	.6984

Table III. Continued

n, rpm	M_t	J	C_T
Run 109			
6 794	0.3204	1.4140	0.4629
8 570	.4041	1.1233	.5581
9 518	.4487	1.0057	.5936
10 462	.4932	.9150	.6225
11 226	.5292	.8544	.6372
11 918	.5618	.8048	.6523
12 332	.5846	.7750	.6602
12 908	.6119	.7403	.6695
15 038	.7128	.6330	.6901
Run 110			
5 506	0.2596	1.4173	0.4697
6 690	.3154	1.1734	.5584
7 368	.3474	1.0683	.5819
8 502	.4009	.9178	.6214
9 160	.4319	.8520	.6427
9 760	.4602	.7995	.6552
10 096	.4784	.7713	.6610
10 522	.4985	.7402	.6710
12 182	.5772	.6411	.6900
14 730	.6980	.5272	.7011
Run 111			
5 376	0.2535	1.4597	0.4810
6 766	.3191	1.1598	.5630
7 502	.3539	1.0458	.6018
8 586	.4050	.9137	.6347
9 224	.4351	.8529	.6524
9 594	.4526	.8106	.6633
10 072	.4775	.7706	.6699
10 508	.4981	.7387	.6765
12 280	.5821	.6338	.6943
14 586	.6914	.5306	.7021
Run 136			
7 638	0.3595	1.4388	0.4600
9 832	.4626	1.1199	.5665
10 646	.5009	1.0359	.5975
12 200	.5738	.9029	.6406
12 930	.6081	.8507	.6540
13 684	.6435	.8039	.6675
14 106	.6695	.7727	.6746
14 182	.6729	.7687	.6740
14 762	.7004	.7375	.6797

Table III. Continued

n, rpm	M_t	J	C_T
Run 137			
6 780	0.3188	1.4065	0.4996
8 320	.3913	1.1417	.5766
9 280	.4364	1.0235	.6050
10 578	.4974	.9014	.6416
11 152	.5245	.8517	.6538
11 840	.5568	.8038	.6677
12 274	.5820	.7690	.6763
12 842	.6090	.7377	.6855
14 672	.6958	.6444	.6992
Run 138			
5 342	0.2514	1.4447	0.5121
6 778	.3189	1.1419	.6041
7 548	.3551	1.0284	.6292
8 306	.3908	.9318	.6485
8 616	.4055	.9009	.6583
9 162	.4312	.8496	.6731
9 620	.4527	.8091	.6807
10 044	.4763	.7669	.6863
10 524	.4991	.7297	.6937
12 136	.5755	.6346	.7076
14 510	.6881	.5308	.7135
Run 139			
9 608	0.4524	1.1441	0.0908
10 046	.4729	1.0944	.1233
10 876	.5119	1.0110	.1630
12 068	.5677	.9116	.2081
12 898	.6068	.8529	.2393
13 710	.6449	.8013	.2629
14 230	.6754	.7651	.2764
14 746	.6998	.7384	.2886
17 248	.8185	.6323	.3381
Run 140			
7 528	0.3541	1.2646	−0.0034
8 376	.3939	1.1366	.0773
9 444	.4442	1.0080	.1572
10 500	.4938	.9085	.2120
11 312	.5320	.8433	.2473
11 784	.5541	.8096	.2642
12 406	.5882	.7612	.2829
12 838	.6087	.7356	.2938
14 916	.7072	.6344	.3371
15 932	.7554	.5928	.3572

Table III. Continued

n, rpm	M_t	J	C_T
Run 141			
6 400	0.3010	1.2069	0.0348
6 772	.3186	1.1438	.0828
7 798	.3668	.9905	.1726
8 574	.4034	.9008	.2229
9 118	.4289	.8495	.2513
9 630	.4530	.8043	.2746
9 928	.4670	.7801	.2871
10 484	.4969	.7332	.3015
12 240	.5802	.6299	.3407
14 682	.6960	.5280	.3902
Run 161			
9 490	0.4376	1.1967	0.0494
10 280	.4739	1.1035	.1100
11 260	.5190	1.0061	.1611
12 528	.5774	.9045	.2131
13 296	.6127	.8536	.2373
14 184	.6535	.8014	.2590
14 554	.6773	.7722	.2689
14 906	.6936	.7540	.2766
15 800	.7352	.7135	.2957
Run 162			
9 462	0.4358	1.2000	0.0282
10 322	.4754	1.0985	.0954
11 248	.5181	1.0111	.1481
12 564	.5786	.9039	.2072
13 298	.6123	.8541	.2335
14 116	.6500	.8047	.2555
14 568	.6776	.7719	.2677
14 888	.6925	.7553	.2758
15 850	.7372	.7105	.2956
Run 163			
8 246	0.3798	1.1954	0.0349
8 910	.4104	1.1084	.0916
9 876	.4549	1.0000	.1613
10 876	.5010	.9080	.2121
11 496	.5295	.8590	.2357
12 318	.5673	.8002	.2642
12 710	.5909	.7697	.2735
12 986	.6038	.7520	.2817
15 168	.7052	.6463	.3279

Table III. Concluded

n, rpm	M_t	J	C_T
Run 164			
8 222	0.3787	1.1988	0.0401
8 922	.4110	1.1005	.1029
9 754	.4493	1.0067	.1547
10 862	.5003	.9057	.2148
11 548	.5319	.8519	.2419
12 262	.5648	.8024	.2650
12 570	.5789	.7827	.2730
12 826	.5963	.7613	.2799
15 160	.7049	.6440	.3304
Run 165			
6 612	0.3046	1.2173	0.0421
7 084	.3264	1.1361	.0913
7 738	.3566	1.0399	.1501
8 778	.4045	.9141	.2208
9 498	.4378	.8423	.2598
9 988	.4603	.8010	.2791
10 306	.4791	.7719	.2838
10 524	.4892	.7559	.2929
12 402	.5765	.6451	.3390
14 760	.6862	.5404	.3805
15 832	.7361	.5052	.3954
Run 166			
6 606	0.3045	1.2109	0.0433
7 188	.3313	1.1129	.1014
7 854	.3621	1.0184	.1560
8 826	.4068	.9063	.2217
9 406	.4336	.8504	.2546
9 980	.4600	.8015	.2751
10 338	.4806	.7693	.2878
10 544	.4902	.7542	.2953
12 284	.5711	.6493	.3355
14 790	.6877	.5408	.3808
15 814	.7353	.5015	.3986

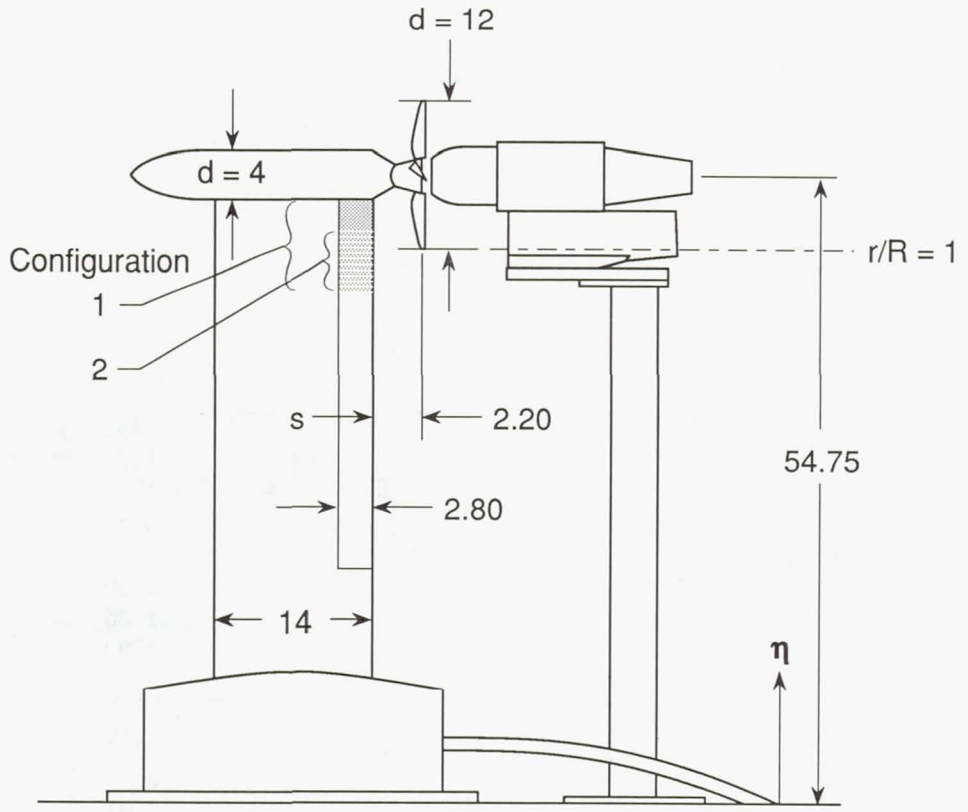

Figure 1. Sketch of propeller/nacelle system and pylon arrangement. All linear dimensions are given in inches.

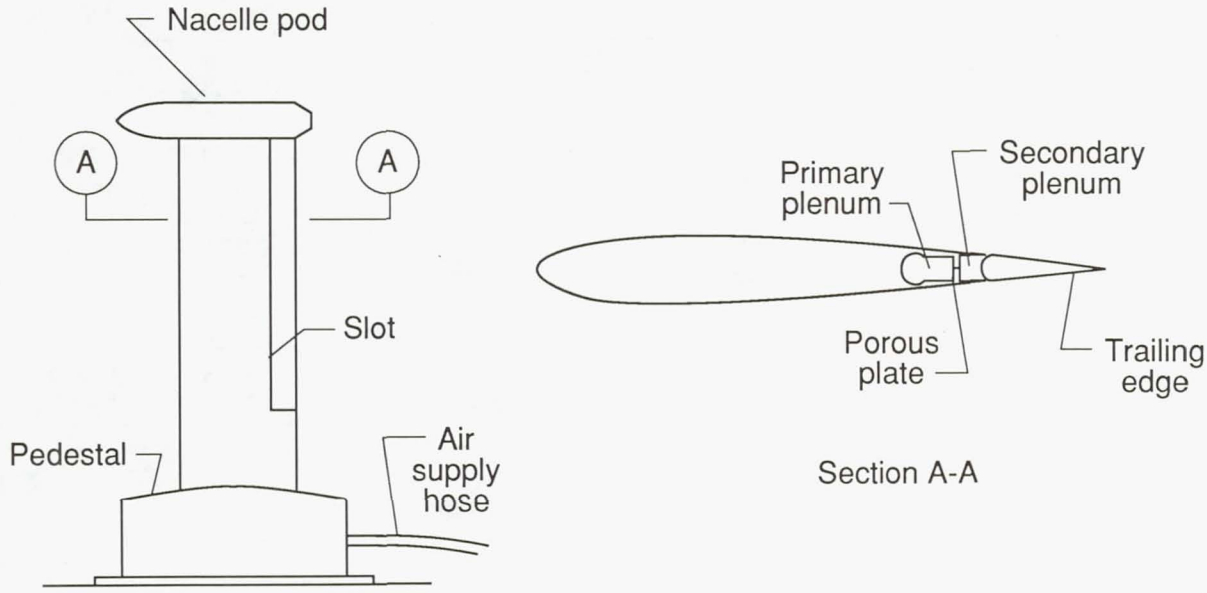

Figure 2. Details of pylon model.

L-87-4725

Figure 3. Photograph of total pressure rake.

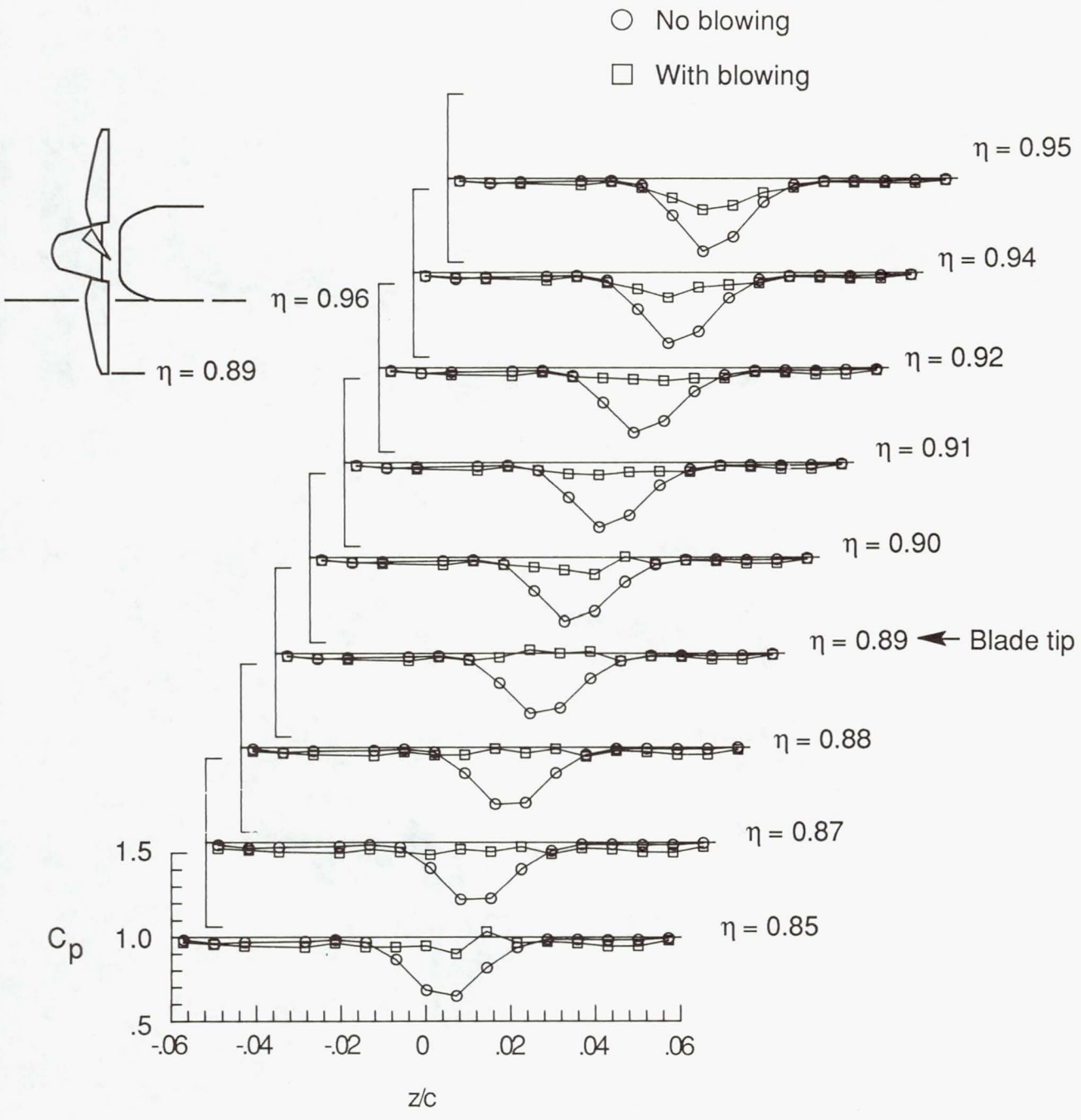

Figure 4. Wake pressure survey of configuration 1 with $q_\infty = 20$ psf.

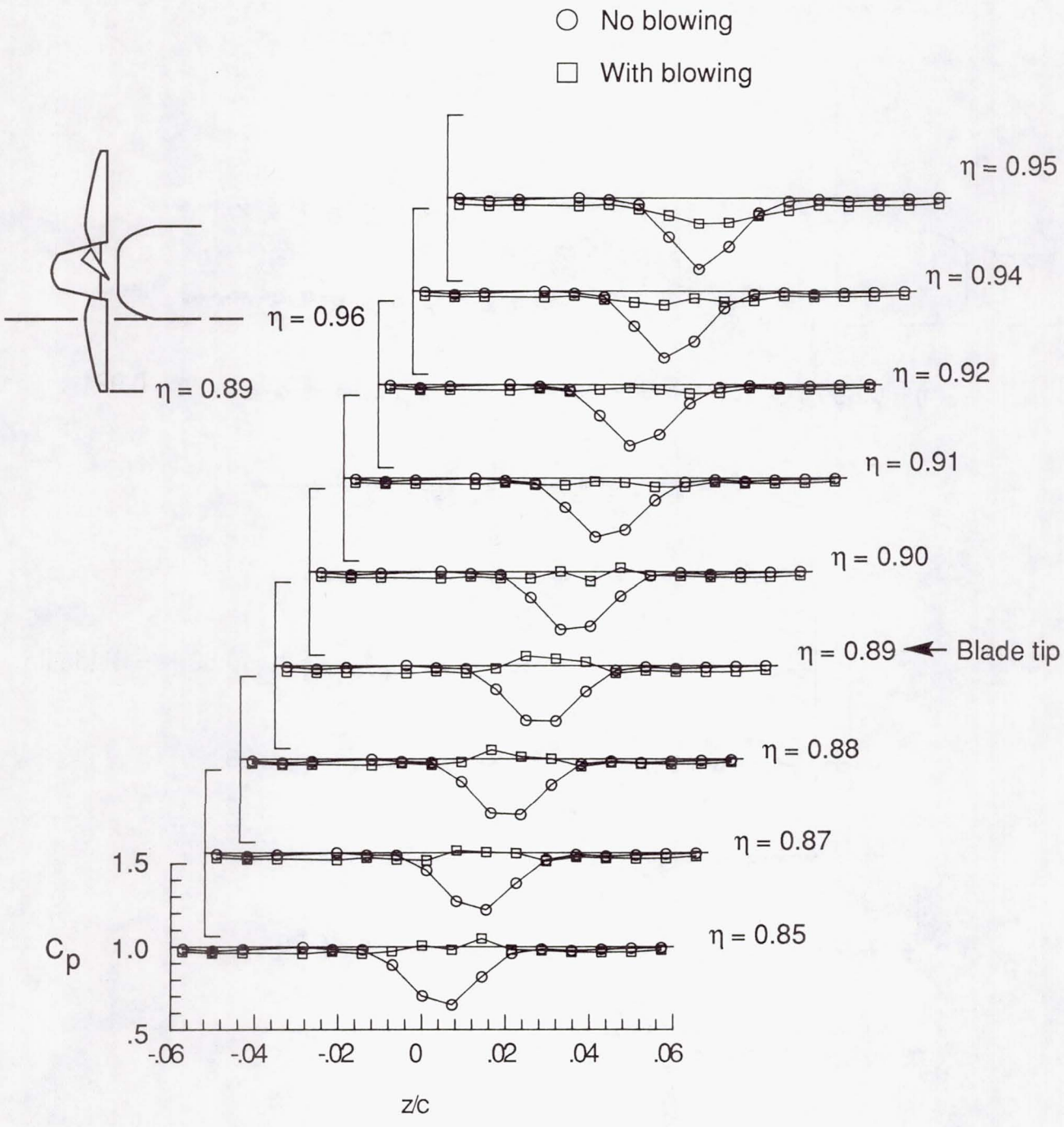

Figure 5. Wake pressure survey of configuration 1 with $q_\infty = 30$ psf.

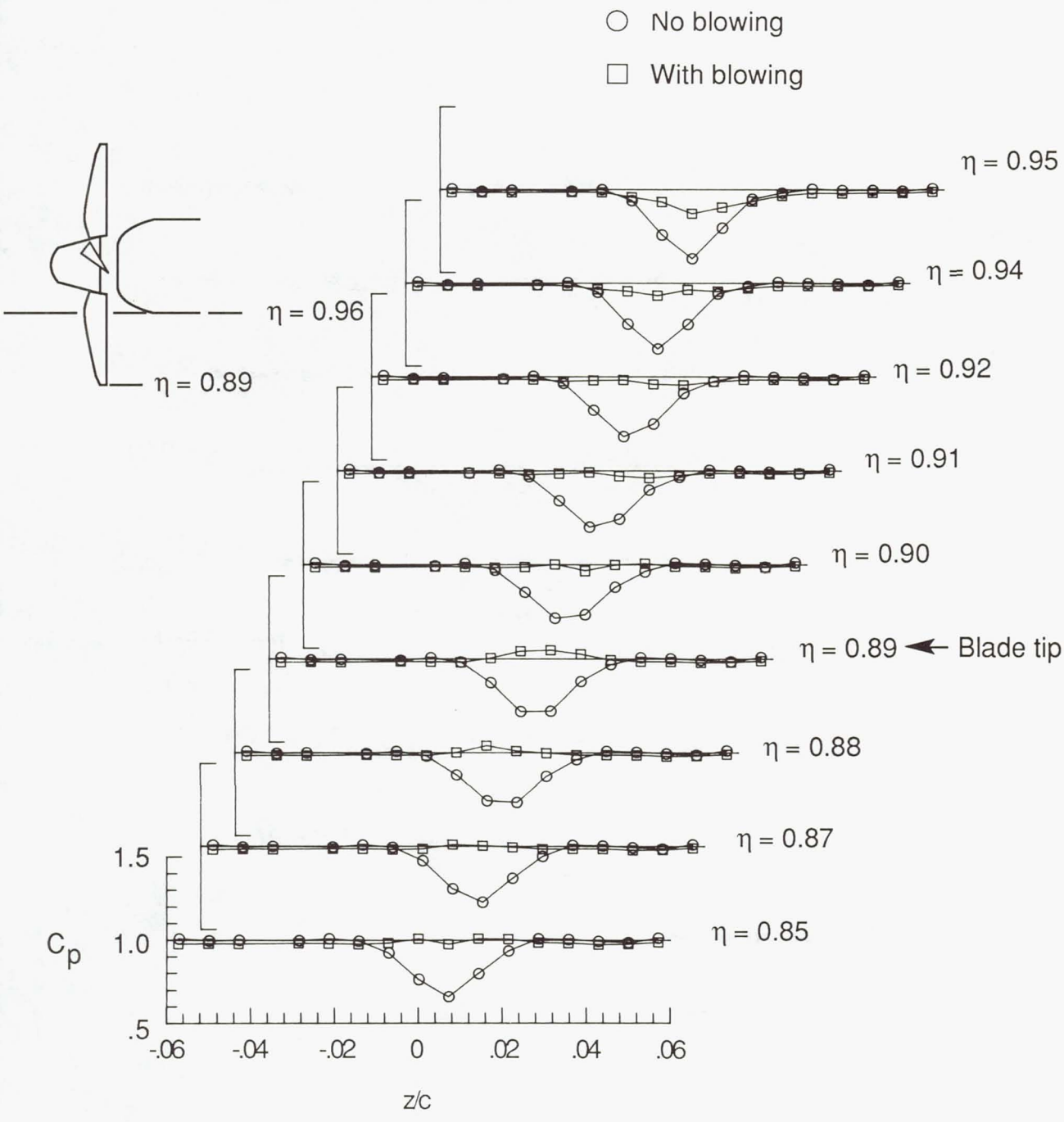

Figure 6. Wake pressure survey of configuration 1 with $q_\infty = 40$ psf.

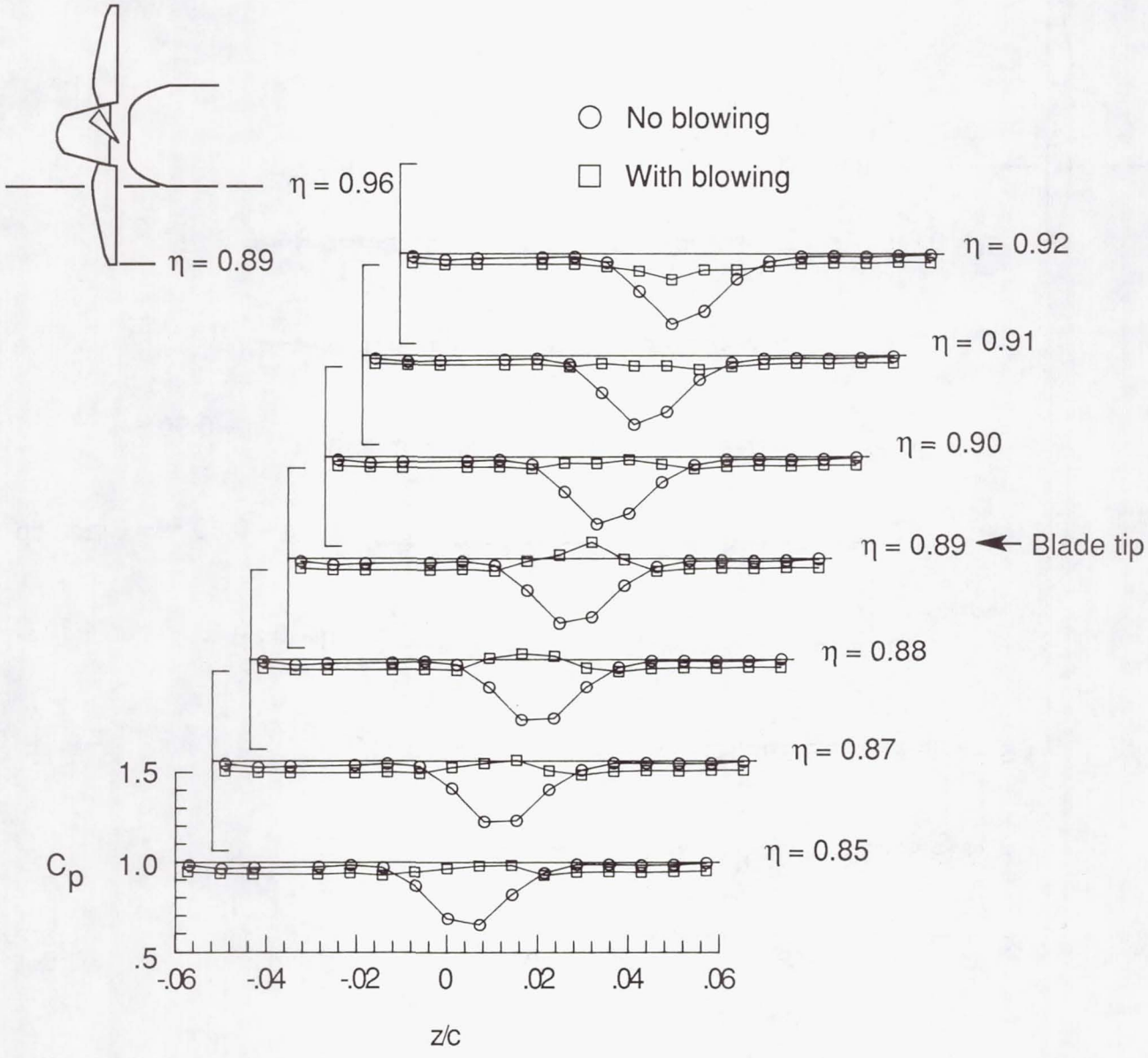

Figure 7. Wake pressure survey of configuration 2 with $q_\infty = 20$ psf.

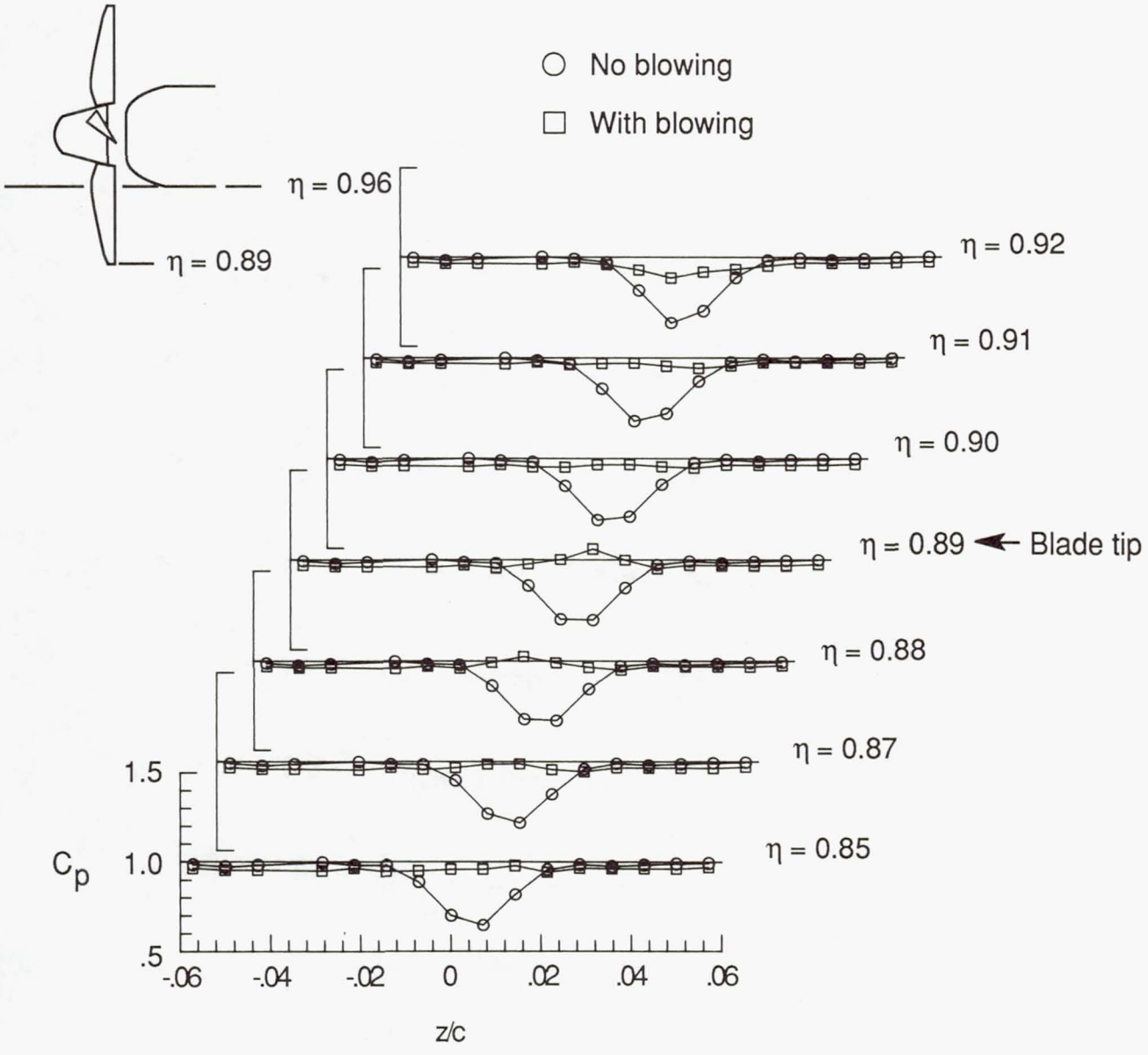

Figure 8. Wake pressure survey of configuration 2 with $q_\infty = 30$ psf.

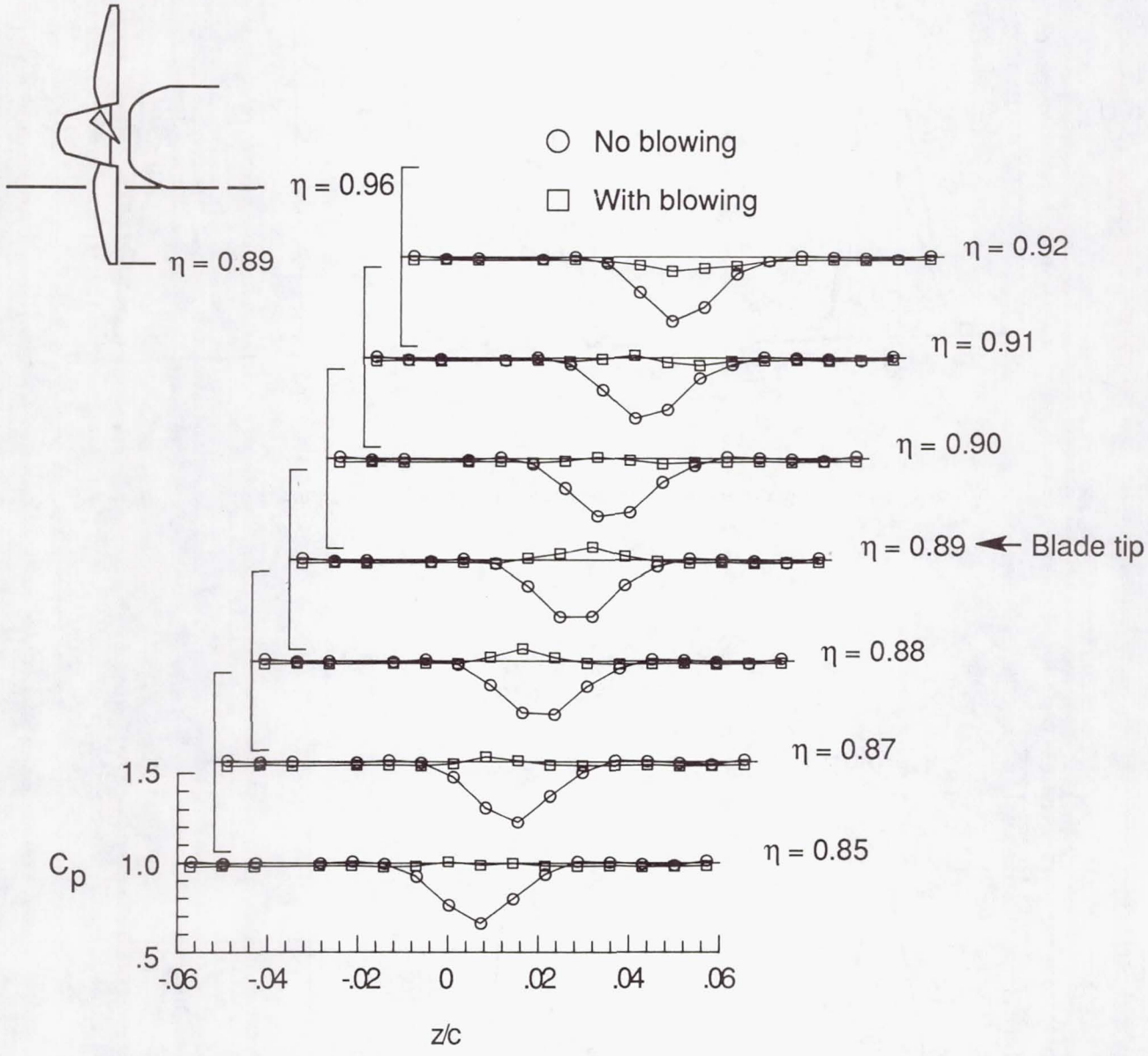

Figure 9. Wake pressure survey of configuration 2 with $q_\infty = 40$ psf.

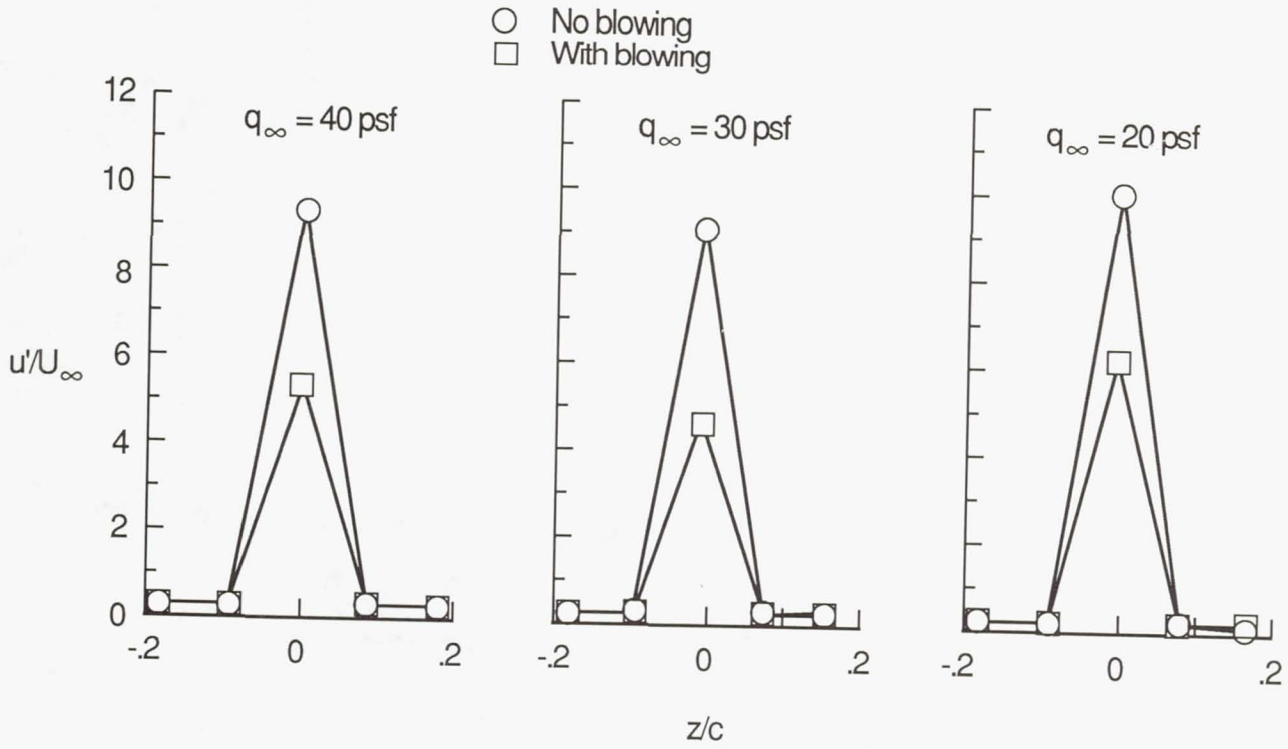

Figure 10. Effect of pylon blowing on wake turbulence intensity for configuration 1 with $\eta = 0.918$.

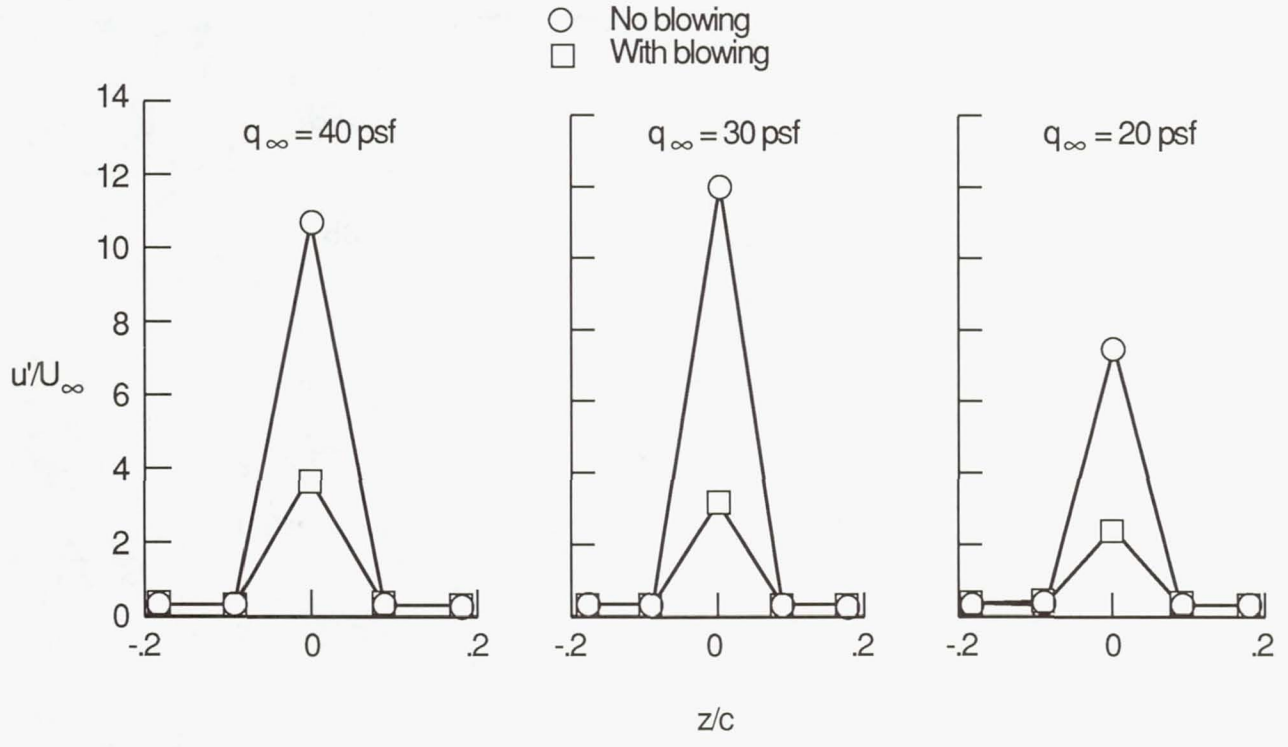

Figure 11. Effect of pylon blowing on wake turbulence intensity for configuration 2 with $\eta = 0.918$.

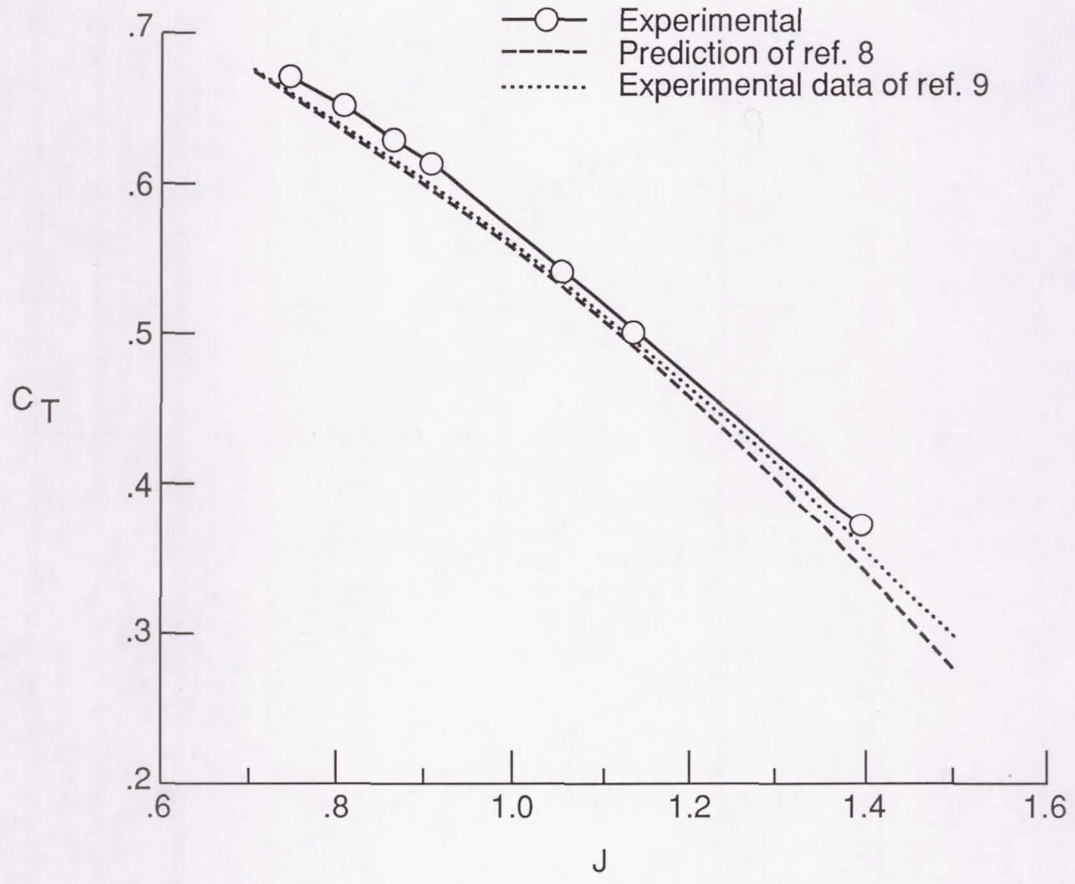

Figure 12. Comparison of calculated and measured thrust coefficients as a function of advance ratio for isolated nacelle with $q_\infty = 40$ psf and $\beta_{.75} = 40°$.

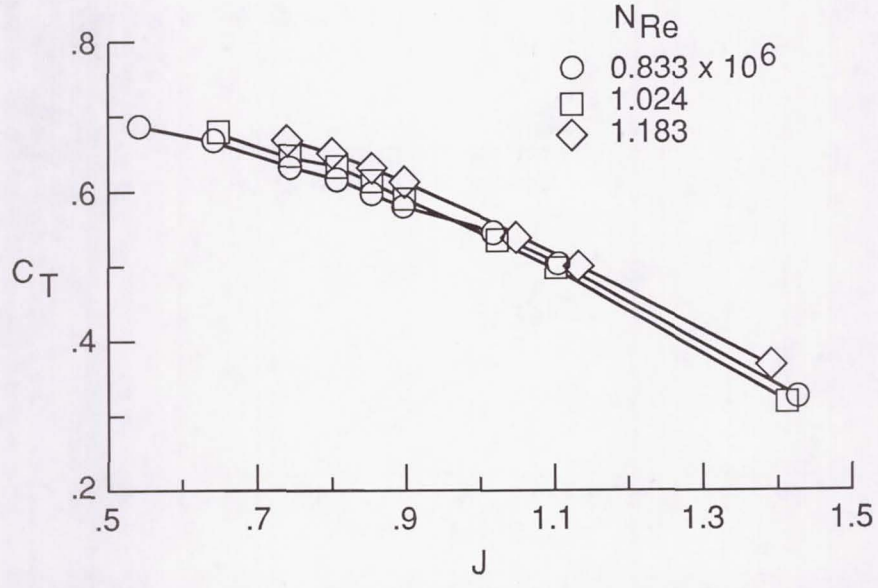

Figure 13. Reynolds number effect on thrust coefficient for isolated nacelle with $\beta_{.75} = 40°$.

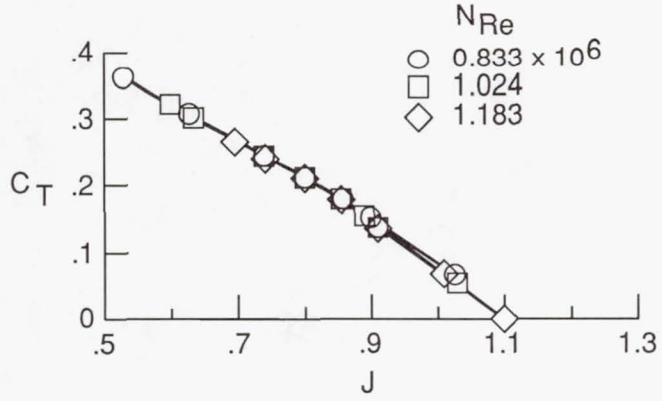

Figure 14. Reynolds number effect on thrust coefficient for isolated nacelle with $\beta_{.75} = 25°$.

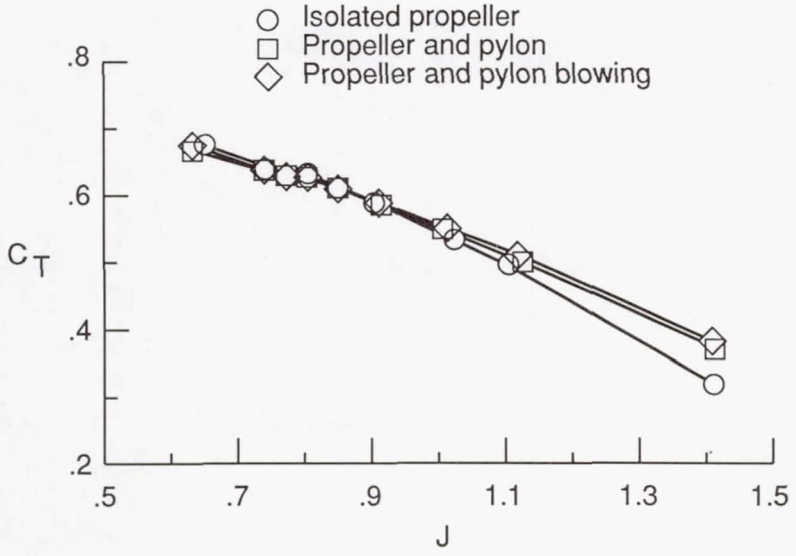

Figure 15. Effect of pylon and pylon blowing on propeller thrust coefficient as a function of advance ratio for configuration 1 with $q_\infty = 30$ psf and $\beta_{.75} = 40°$.

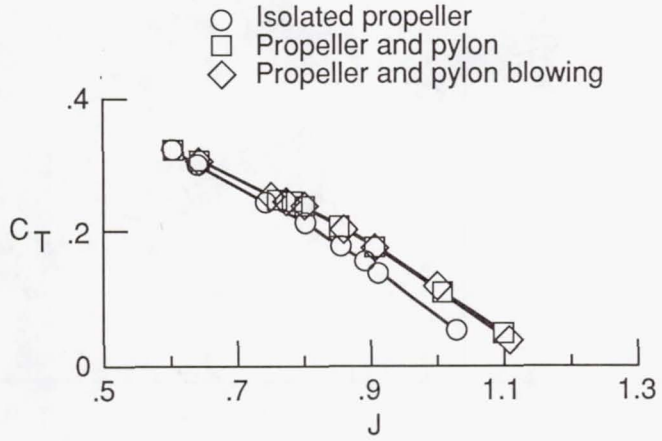

Figure 16. Effect of pylon and pylon blowing on propeller thrust coefficient as a function of advance ratio for configuration 1 with $q_\infty = 30$ psf and $\beta_{.75} = 25°$.

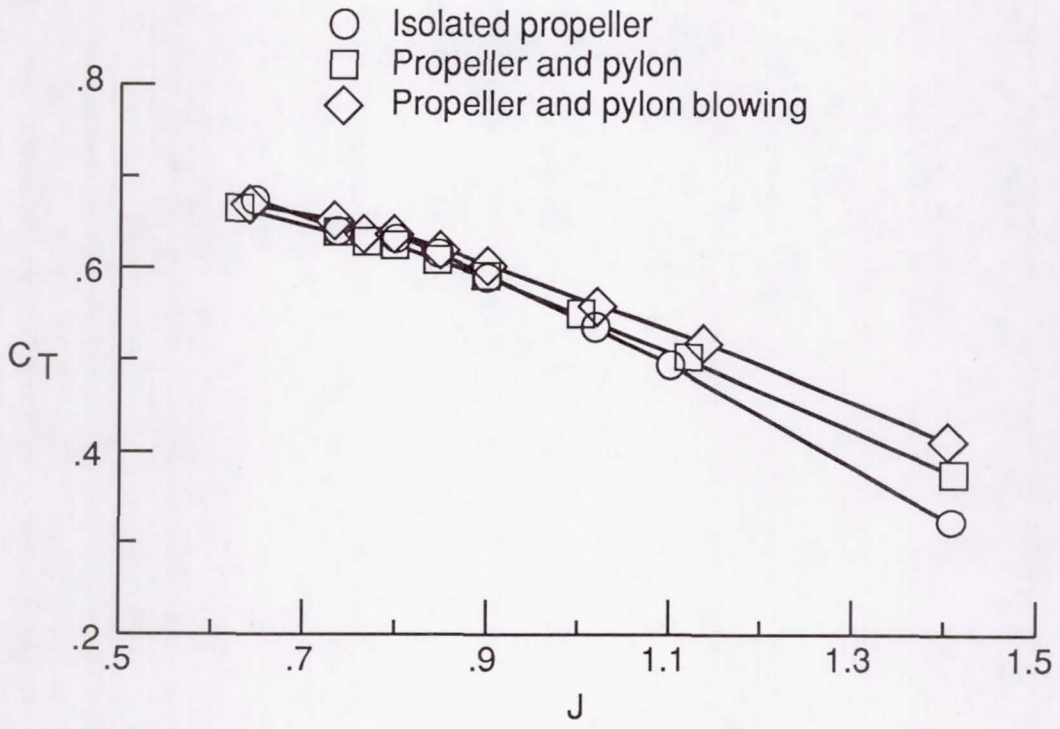

Figure 17. Effect of pylon and pylon blowing on propeller thrust coefficient as a function of advance ratio for configuration 2 with $q_\infty = 30$ psf and $\beta_{.75} = 40°$.

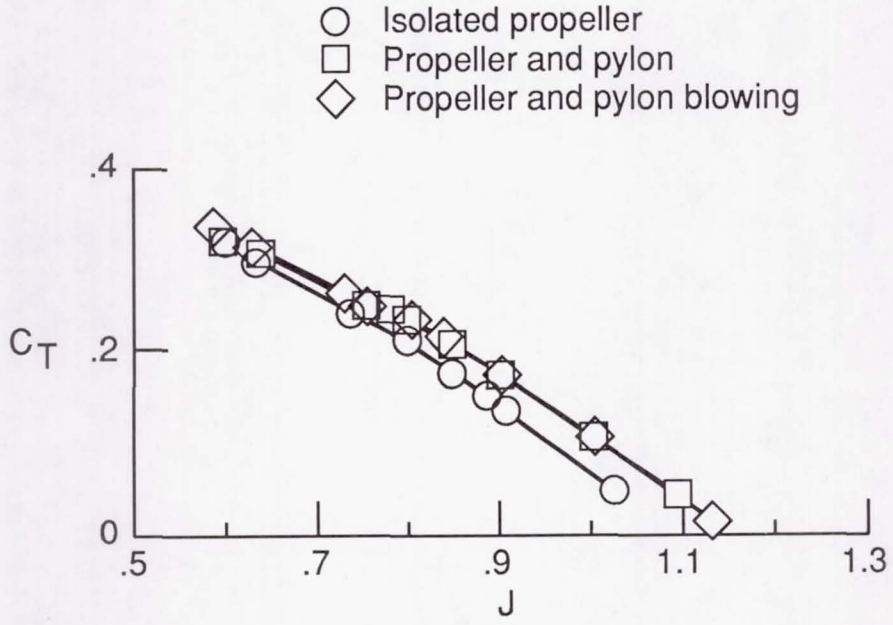

Figure 18. Effect of pylon and pylon blowing on propeller thrust coefficient as a function of advance ratio for configuration 2 with $q_\infty = 30$ psf and $\beta_{.75} = 25°$.

NASA
National Aeronautics and Space Administration

Report Documentation Page

1. Report No.	2. Government Accession No.	3. Recipient's Catalog No.
NASA TM-4162		

4. Title and Subtitle	5. Report Date
Effect of Pylon Wake With and Without Pylon Blowing on Propeller Thrust	February 1990
	6. Performing Organization Code
7. Author(s)	8. Performing Organization Report No.
Garl L. Gentry, Jr., Earl R. Booth, Jr., and M. A. Takallu	L-16645
9. Performing Organization Name and Address	10. Work Unit No.
NASA Langley Research Center Hampton, VA 23665-5225	535-03-01-02
	11. Contract or Grant No.
12. Sponsoring Agency Name and Address	13. Type of Report and Period Covered
National Aeronautics and Space Administration Washington, DC 20546-0001	Technical Memorandum
	14. Sponsoring Agency Code

15. Supplementary Notes

Garl L. Gentry, Jr., and Earl R. Booth, Jr.: Langley Research Center, Hampton, Virginia.
M. A. Takallu: PRC Kentron, Inc., Aerospace Technologies Division, Hampton, Virginia.

16. Abstract

Pylon trailing-edge blowing has been investigated as a means of alleviating the effects of the pylon wake on a pusher arrangement of an advanced single-rotation turboprop. Measurements were made of the steady-state propeller thrust and pylon-wake pressure distribution and turbulence level with and without blowing. Results showed pylon trailing-edge blowing practically eliminated the pylon wake, significantly reduced the pylon-wake turbulence, and had a relatively small effect on the steady-state propeller thrust. The data are presented with a minimum of analysis.

17. Key Words (Suggested by Authors(s))	18. Distribution Statement
Turboprop Single-rotation propeller Pusher propeller Blown pylon	Unclassified—Unlimited Subject Category 02

19. Security Classif. (of this report)	20. Security Classif. (of this page)	21. No. of Pages	22. Price
Unclassified	Unclassified	24	A03

NASA-Langley, 1990

For sale by the National Technical Information Service, Springfield, Virginia 22161-2171